ResearchGate

See discussions, stats, and author profiles for this publication at: https://www.researchgate.net/publication/322828455

Fourth order Galilean invariance for the lattice Boltzmann method

Article *in* Computers & Fluids · April 2018

DOI: 10.1016/j.compfluid.2018.01.015

CITATIONS
2

READS
88

2 authors:

Martin Geier
Technische Universität Braunschweig
37 PUBLICATIONS **422** CITATIONS
SEE PROFILE

Andrea Pasquali
FluiDyna GmbH
9 PUBLICATIONS **67** CITATIONS
SEE PROFILE

All content following this page was uploaded by Martin Geier on 08 February 2018.

The user has requested enhancement of the downloaded file.

Fourth order Galilean invariance for the lattice Boltzmann method

Martin Geier[a,*], Andrea Pasquali[a,b]

[a]*TU Braunschweig, Institute for Computational Modeling in Civil Engineering (iRMB), Braunschweig, Germany*
[b]*FluiDyna GmbH, Edisonstrasse 3, 85716 Unterschleissheim, Germany*

Abstract

Using the structure of a recursive asymptotic analysis we derive conditions on cumulants that guarantee a prescribed order of Galilean invariance for lattice Boltzmann models. We then apply these conditions to three different lattice Boltzmann models and obtain three model with fourth order accurate advection. One of the models uses 27 speeds on a body centered cubic lattice, one uses 33 speeds on an extended Cartesian lattice and one uses 27 speeds plus three finite differences on a Cartesian lattice. All models offer too few degrees of freedom to impose the conditions on the cumulants directly. However, the specific aliasing structure of these lattices permit fourth order accuracy for a model specific optimal reference temperature. Our theoretical derivations are confirmed by measuring the phase lag of traveling vortexes and shear waves.

Keywords: lattice Boltzmann, cumulants, Galilean invariance, fourth order, crystallographic lattice Boltzmann, recursive asymptotic analysis

1. Introduction

For Eulerian (i.e. fixed grid) methods used in computational fluid mechanics Galilean invariance can, in general, only be obtained within a finite order of approximation. In particular the violations of Galilean invariance in the lattice Boltzmann method are widely discussed in literature [1, 2, 3, 4, 5, 6, 7]. Within the limits of second order accuracy the problem is in general solved. However, beyond the second order there are several spurious dependencies of the solution on the frame of reference. These include: a dependance of the viscosity on the flow speed, spurious couplings between moments relaxing with different relaxation rates (in the case of the multi-relaxation time lattice Boltzmann model), and a phase lag in the advection of vortexes. The first two problems have been solved with the introduction of the cumulant lattice Boltzmann method [6] using a transformation to Galilean invariant mutually uncorrelated observable quantities before collision. What has not yet been solved is the phase lag problem in the advection of traveling vortexes in a superimposed velocity field. This error apparently cannot easily be removed within the usual discretization of the lattice Boltzmann model, at least not without introducing more discrete velocities than usually used.

In order to increase the asymptotic accuracy of the lattice Boltzmann method with regard to Galilean invariance to fourth order all velocity moments up to order four have to be sufficiently Galilean invariant. This implies the application of a very large set of discrete velocities which is undesirable for reasons of efficiency. Instead it is desirable to find a specific discretization that reduces the number of required discrete velocities. This is in theory possible through the aliasing structure of a velocity set. Each finite set of velocities has an infinite number of moments of which only a finite number is independent. In some cases it is possible to design a specific finite velocity set in such a way that the dependent moments turn out to be correct within a required order of accuracy. Hence, in such a case it is not necessary to introduce new variables for additional discrete speeds and the computational efficiency is largely enhanced.

*Corresponding author at: iRMB Pockelsstr. 3, 38106 Braunschweig, Germany. Tel: +49 531 391 94518; Fax: +49 531 391 94511.
Email address: geier@irmb.tu-bs.de (Martin Geier)

In this paper we investigate different possibilities to remove the phase lag Galilean invariance problem of the cumulant lattice Boltzmann method and make the Galilean invariance of the model fourth order accurate. This is done here in three different ways: by using a different arrangement of the discrete speeds than in the original method; by using more speeds; and by using finite differences to repair the original method (hybrid model).

The reminder of the paper is organized as follows: in section two we address the different possibilities to design lattices based on the cubic Bravais lattice structures. Section three introduces the recursive asymptotic analysis technique in diffusive scaling (where we assume that the time step scales with the square of the grid spacing) used for deriving equivalent partial differential equations of the lattice Boltzmann method. In section four we give a brief introduction to cumulants. In section five we derive conditions for Galilean invariance based on the results of the previous two sections. Section six introduces the hybrid model. Section seven discusses some implementation issues of the three models. Section eight presents the numerical confirmation of our derivations, followed by section nine with the conclusions.

2. Crystallographic lattice Boltzmann models

The most commonly applied lattice Boltzmann models use a Cartesian distribution of nodes which, in terms of crystallographic unit cells, corresponds to a simple cubic configuration. Recently, Namburi et al. introduced a lattice Boltzmann discretization based on a body centered cubic unit cell and called this method "crystallographic" lattice Boltzmann [8] arguing that it was inspired from the Bravais lattices used in crystallographic theory [9]. However, we will call Namburi's lattice body centered cubic (BCC) instead of crystallographic due to the fact that the usual simple cubic (SC) discretization is a Bravais lattice too. Yet we stick to the nomenclature of [8] and refer to the velocity distribution of the BCC lattice by RD3Q27 to distinguish it from the Cartesian lattice Boltzmann velocity distribution using 27 speed (D3Q27).

All possible space filling crystallographic lattices can be classified into 14 Bravais lattices of which only three are cubic and hence of interest for approximately isotropic discretizations (see Fig. 1). These are the simple cubic (SC) lattice, the body centered cubic (BCC) lattice and the face centered cubic (FCC) lattice. All three lattices have been used as the basis for lattice Boltzmann models. The popular standard Cartesian lattices with 15, 19 and 27 speeds in three dimensions are SC lattices. Namburi's method uses 27 speeds on a BCC lattice and the so called D3Q13 method uses a FCC lattice [10, 11, 12].

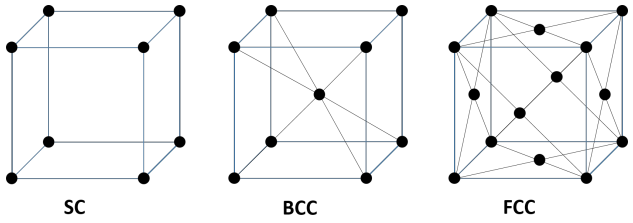

Figure 1: The three cubic Bravais lattices from left to right: simple cubic (SC), body centered cubic (BCC), and face centered cubic (FCC). These three lattices represent all possible periodic configurations of space filling cubic arrangements of nodes. The simple cubic lattice represents the Cartesian case which is used in most lattice Boltzmann methods. The other two cases have also been used for lattice Boltzmann models: the body centered cubic lattice in Namburi's RD3Q27 method [8] and the face centered cubic lattice in the d'Humières D3Q13 method [10].

According to the theory of Bravais lattices there is nothing beyond this three possibilities, unless unsymmetrical lattices would be considered.

We observed in the past that the standard cumulant lattice Boltzmann method with 27 speeds on a SC lattice lacks Galilean invariance of fourth order only in certain directions [6]. We conjectured that a BCC lattice with the same number of speeds could be more isotropic and should hence be a better starting point for a complete fulfillment of fourth order accuracy of the Galilean invariance. We will therefore investigate the lattice structure proposed by Namburi et al. [8]. In addition, we use a model with 33 speeds on a Cartesian grid to enforce Galilean invariance. We also propose one additional model supplementing the standard D3Q27 lattice with three finite differences to obtain Galilean invariance at fourth order. All lattice used in this study are shown in Fig. 2.

For giving an explicit definition of the used velocity models we introduce the following energy shells:

$$
\begin{aligned}
E_0 &= \{0,0,0\}, && (1)\\
E_1 &= \{0,0,\pm1\} \cup \{0,\pm1,0\} \cup \{\pm1,0,0\}, && (2)\\
E_{\sqrt{2}} &= \{0,\pm1,\pm1\} \cup \{\pm1,0,\pm1\} \cup \{\pm1,\pm1,0\}, && (3)\\
E_{\sqrt{3}} &= \{\pm1,\pm1,\pm1\}, && (4)\\
E_{\sqrt{3/4}} &= \{\pm1/2,\pm1/2,\pm1/2\}, && (5)\\
E_2 &= \{0,0,\pm2\} \cup \{0,\pm2,0\} \cup \{\pm2,0,0\}. && (6)
\end{aligned}
$$

The SC D3Q27 lattice uses the velocity set $\{i,j,k\}_{D3Q27} \in E_0 \cup E_1 \cup E_{\sqrt{2}} \cup E_{\sqrt{3}}$. The BCC lattice uses the set $\{i,j,k\}_{RD3Q27} \in E_0 \cup E_1 \cup E_{\sqrt{2}} \cup E_{\sqrt{3/4}}$ and the D3Q33 lattice the set $\{i,j,k\}_{D3Q33} \in E_0 \cup E_1 \cup E_{\sqrt{2}} \cup E_{\sqrt{3}} \cup E_2$. The D3Q27F3 lattice uses the same velocity set as the D3Q27 lattice plus three simple finite difference stencils.

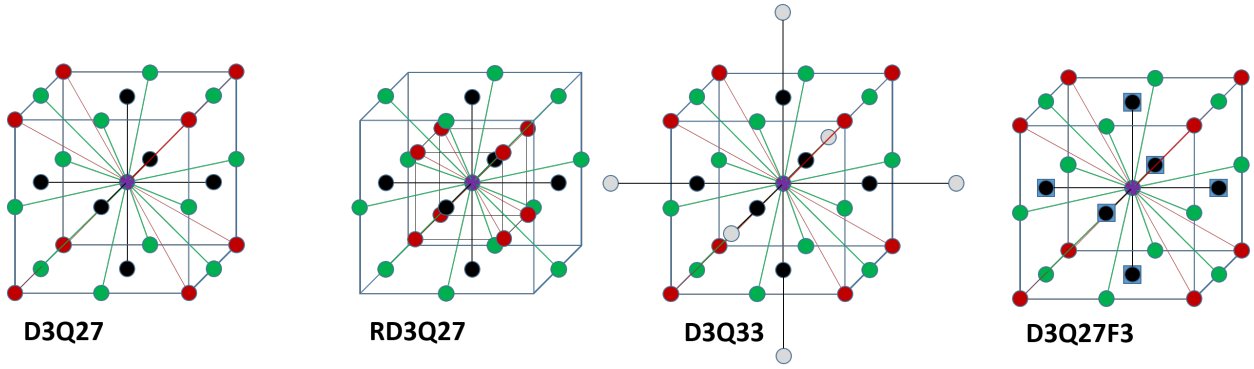

Figure 2: The four different velocity lattices used in this study. The two lattices on the left have 27 degrees of freedom each. The two lattices on right have 33 degrees of freedom. The D3Q27F3 lattice is a hybrid model that uses 27 distributions together with six pseudo distributions (indicated by squares) used to compute finite differences.

3. Recursive asymptotic analysis

For the assessment of the convergence order of the lattice Boltzmann method, the rigorous approach is to apply an asymptotic expansion to the lattice Boltzmann equation [13]. The lattice Boltzmann equation for the pre-collision particle velocity distribution function $f_{ijkxyzt}$ can be written as:

$$
f^*_{ijk(x-ic\Delta t/2)(y-jc\Delta t/2)(z-kc\Delta t/2)(t-\Delta t/2)} - f_{ijk(x+ic\Delta t/2)(y+jc\Delta t/2)(z+kc\Delta t/2)(t+\Delta t/2)} = 0. \tag{7}
$$

With the lattice speed $c = \Delta x/\Delta t$ and i, j and k being the quantum numbers for particles moving in x, y and z direction. The range of the quantum numbers depend on the velocity set. The asterisk indicates the post-collision state. In order to eliminate the pre- and post-collision states and to introduce the collision operator in distribution form $\Omega^{\mathrm{f}}_{ijkxyzt}$ we define [14, 15]:

$$
\begin{aligned}
f_{ijkxyzt} &= \bar{f}_{ijkxyzt} - \Omega^{\mathrm{f}}_{ijkxyzt}/2, && (8)\\
f^*_{ijkxyzt} &= \bar{f}_{ijkxyzt} + \Omega^{\mathrm{f}}_{ijkxyzt}/2. && (9)
\end{aligned}
$$

With this Eq. (7) becomes:

$$
\begin{aligned}
0 = {} & -\bar{f}_{ijk(x+ic\Delta t/2)(y+jc\Delta t/2)(z+kc\Delta t/2)(t+\Delta t/2)} + \bar{f}_{ijk(x-ic\Delta t/2)(y-jc\Delta t/2)(z-kc\Delta t/2)(t-\Delta t/2)}\\
& + \Omega^{\mathrm{f}}_{ijk(x+ic\Delta t/2)(y+jc\Delta t/2)(z+kc\Delta t/2)(t+\Delta t/2)}/2 + \Omega^{\mathrm{f}}_{ijk(x-ic\Delta t/2)(y-jc\Delta t/2)(z-kc\Delta t/2)(t-\Delta t/2)}/2. \qquad (10)
\end{aligned}
$$

The Taylor expansion [16] of Eq. (10) is seen to have the nice property that the distributions vanish at all even orders and the collision operator vanishes at all odd orders in the expansion parameter Δt:

$$0 = \sum_{m,n,o,q=0}^{\infty} \frac{\partial_x^m \partial_y^n \partial_z^o \partial_t^q}{m!n!o!q!} \left(\left(\frac{\Delta t}{2} \right)^{m+n+o+q} c^{m+n+o} i^m j^n k^o \right) \left(\bar{f}_{ijkxyzt} \left((-1)^{m+n+o+q} - 1 \right) + \frac{\Omega^{\mathrm{f}}_{ijkxyzt}}{2} \left(1 + (-1)^{m+n+o+q} \right) \right). \tag{11}$$

We define the countable raw moments omitting the time and space variables from here on:

$$\bar{m}_{\alpha\beta\gamma} = \sum_{i,j,k} i^\alpha j^\beta k^\gamma \bar{f}_{ijk}. \tag{12}$$

The sum of the indexes of a moment $\alpha + \beta + \gamma$ is refered to as the order of the moment. We can rewrite Eq. (11) by substituting the distributions by Eq. (12) and by using the collision operator in moment form $\Omega^{\mathrm{m}}_{ijk}$:

$$0 = \sum_{m,n,o,q=0}^{\infty} \frac{\partial_x^m \partial_y^n \partial_z^o \partial_t^q}{m!n!o!q!} \left(\frac{\Delta t c}{2} \right)^{m+n+o+q} \frac{1}{c^q} \left(\bar{m}_{(\alpha+m)(\beta+n)(\gamma+o)} \left((-1)^{m+n+o+q} - 1 \right) + \frac{\Omega^{\mathrm{m}}_{(\alpha+m)(\beta+n)(\gamma+o)}}{2} \left(1 + (-1)^{m+n+o+q} \right) \right). \tag{13}$$

Recalling that $c = \Delta x / \Delta t$ we see that this equation has two independent smallness parameters. In order to derive the asymptotic limit we have to decide on a scaling between them. Here we use the diffusive scaling such that $\Delta t \to \epsilon^2$ and $\Delta t c = \Delta x \to \epsilon$. Eq. (13) hence becomes:

$$0 = \sum_{m,n,o,q=0}^{\infty} \frac{\partial_x^m \partial_y^n \partial_z^o \partial_t^q}{m!n!o!q!} \frac{\epsilon^{2q+m+n+o}}{2^{m+n+o+q}} \left(\bar{m}_{(\alpha+m)(\beta+n)(\gamma+o)} \left((-1)^{m+n+o+q} - 1 \right) + \frac{\Omega^{\mathrm{m}}_{(\alpha+m)(\beta+n)(\gamma+o)}}{2} \left(1 + (-1)^{m+n+o+q} \right) \right). \tag{14}$$

Finally we expand the moments and the collision operator in terms of the smallness parameter ϵ:

$$m_{\alpha\beta\gamma} = \sum_{r=0}^{\infty} \epsilon^r m^{(r)}_{\alpha\beta\gamma}, \tag{15}$$

$$\Omega^{\mathrm{m}}_{\alpha\beta\gamma} = \sum_{r=0}^{\infty} \epsilon^r \Omega^{\mathrm{m}(r)}_{\alpha\beta\gamma}, \tag{16}$$

and introduce the expanded forms into Eq. (14):

$$0 = \sum_{m,n,o,q,r=0}^{\infty} \frac{\partial_x^m \partial_y^n \partial_z^o \partial_t^q}{m!n!o!q!} \frac{\epsilon^{2q+r+m+n+o}}{2^{m+n+o+q}} \left(\bar{m}^{(r)}_{(\alpha+m)(\beta+n)(\gamma+o)} \left((-1)^{m+n+o+q} - 1 \right) + \frac{\Omega^{\mathrm{m}(r)}_{(\alpha+m)(\beta+n)(\gamma+o)}}{2} \left(1 + (-1)^{m+n+o+q} \right) \right). \tag{17}$$

The sum in Eq. (17) is zero for arbitrary $\epsilon > 0$ if and only if each order in ϵ is zero individually such that we can equate coefficients:

$$0 = \sum_{m,n,o,q=0}^{r} \frac{\partial_x^m \partial_y^n \partial_z^o \partial_t^q}{m!n!o!q!} \frac{1}{2^{m+n+o+q}} \left(\bar{m}^{(r-2q-o-n-m)}_{(\alpha+m)(\beta+n)(\gamma+o)} \left((-1)^{m+n+o+q} - 1 \right) + \frac{\Omega^{\mathrm{m}(r-2q-o-m-n)}_{(\alpha+m)(\beta+n)(\gamma+o)}}{2} \left(1 + (-1)^{m+n+o+q} \right) \right). \tag{18}$$

Here we assume that all negative orders of the moments and the collision operator vanish (that is if $r-2q-o-n-m < 0$). This is also why the sum only needs to be evaluated until r. Eq. (18) can now be solved for $\Omega^{\mathrm{m}(r)}_{\alpha\beta\gamma}$:

$$\Omega^{\mathrm{m}(r)}_{\alpha\beta\gamma} = - \sum_{\substack{m,n,o,q=0 \\ 2q+o+m+n \neq 0}}^{r} \frac{\partial_x^m \partial_y^n \partial_z^o \partial_t^q}{m!n!o!q!} \frac{1}{2^{m+n+o+q}} \left(\bar{m}^{(r-2q-o-n-m)}_{(\alpha+m)(\beta+n)(\gamma+o)} \left((-1)^{m+n+o+q} - 1 \right) + \frac{\Omega^{\mathrm{m}(r-2q-o-m-n)}_{(\alpha+m)(\beta+n)(\gamma+o)}}{2} \left(1 + (-1)^{m+n+o+q} \right) \right). \tag{19}$$

Eq. (19) is a recursive asymptotic expansion [17]. Since all negative orders of the collision operator vanish it is always possible for any finite and positive order r to eliminate the collision operator from the right hand side of Eq. (19) by repeatedly inserting Eq. (19) into itself. Once this is accomplished the resulting $\Omega^{\mathrm{m}(r)}_{\alpha\beta\gamma}$ can be inserted into Eq. (18) to eliminate the collision operator. This has the advantage to make the expansion entirely independent of both the collision operator and the lattice structure. The bared moments are related to the pre-collision moments $m_{\alpha\beta\gamma}$ and the post-collision moments $m^*_{\alpha\beta\gamma}$ by:

$$\bar{m}_{\alpha\beta\gamma} = m_{\alpha\beta\gamma} + \Omega^{\mathrm{m}}_{\alpha\beta\gamma}/2, \tag{20}$$

$$\bar{m}_{\alpha\beta\gamma} = m^*_{\alpha\beta\gamma} - \Omega^{\mathrm{m}}_{\alpha\beta\gamma}/2. \tag{21}$$

The collision operator is hence seen to be reintroduced through the bared moments.

The lattice structure is also implicitly present in the expansion via the moments. Any lattice with a finite set of discrete velocities will only produce the same number of independent moments. Here lays the principle difference between the Cartesian D3Q27 lattice and the body centered cubic RD3Q27 lattice. The Cartesian lattice has a very simple aliasing structure in which the moments just reappear such that $m^{D3Q27}_{300} = m^{D3Q27}_{100}$, $m^{D3Q27}_{400} = m^{D3Q27}_{200}$, $m^{D3Q27}_{310} = m^{D3Q27}_{110}$ and so on. The aliasing on the body centered cubic grid is much more complicated. There we have m_{300} as an independent moment but the dependent moments have a more complicated relationship with the independent moments:

$$m^{RD3Q27}_{310} = m^{RD3Q27}_{110} - 3m^{RD3Q27}_{112}, \tag{22}$$

$$m^{RD3Q27}_{400} = \frac{1}{2}(m^{RD3Q27}_{040} + m^{RD3Q27}_{004} + 2m^{RD3Q27}_{200} - m^{RD3Q27}_{002} - m^{RD3Q27}_{020}), \tag{23}$$

$$m^{RD3Q27}_{122} = \frac{1}{12}(m^{RD3Q27}_{100} - m^{RD3Q27}_{300}), \tag{24}$$

$$m^{RD3Q27}_{320} = \frac{1}{4}(-m^{RD3Q27}_{100} + 4m^{RD3Q27}_{120} + m^{RD3Q27}_{300}), \tag{25}$$

$$m^{RD3Q27}_{311} = \frac{m^{RD3Q27}_{111}}{4}. \tag{26}$$

On the D3Q33 lattice both m_{300} and m_{400} are independent moments.

Together with the number of independent moments the aliasing structure dictates the level of accuracy that can be obtained with a given lattice.

In order to derive the equivalent partial differential equations of the lattice Boltzmann model and confirm its order of accuracy with respect to a target equation (which would be the Navier-Stokes equations in our case) it is necessary to insert the actual collision operator and the lattice structure into Eq. (18) for all moments and repeat the insertion recursively until all non-conserved moments are eliminated and the remaining equivalent partial differential equation is only a function of the conserved quantities. To evaluate the convergence order of the method it is necessary to evaluate also the higher orders of the conserved quantities, in particular it is necessary to obtain the partial differential equations of $m^{(3)}_{100}$, $m^{(5)}_{100}$, $\cdots$ and judge whether or not these equations permit null solutions for any admissible solution in the leading order of the conserved quantities ($m^{(1)}_{100}$, $m^{(1)}_{010}$, $m^{(1)}_{001}$ and $m^{(2)}_{000}$). This is a very tedious calculation. Fortunately, in order to judge whether a certain velocity set permits Galilean invariant solution up to a given order, it is not actually necessary to perform the asymptotic analysis to that order. Instead, it is sufficient to exploit the structure of the expansion and apply the theory of cumulants.

4. Cumulants

Cumulants are the statistically independent observable quantities of a distribution. In this context statistical independence between two observable quantities is defined as the property that their joint probability distribution function is the product of their individual distribution functions.

Probability distributions are often expressed in terms of their moments obtained from the moment generating function:

$$M(\Xi) = \int_{-\infty}^{\infty} e^{-\Xi\xi} f(\xi) d\xi = \mathcal{L}(f(\xi)), \tag{27}$$

where ξ is the random variable and $\mathcal{L}$ represents the Laplace transform. For the momentum distribution function in the Boltzmann equation ξ would be the microscopic particle velocity. The moment generating function Eq. (27) can be understood as the Laplace transform of the distribution $f(\xi)$. Moments are obtained by getting successive derivatives of $M(\Xi)$ at $\Xi = 0$, i.e.:

$$m_n = \frac{\partial^n}{\partial \Xi^n} M(\Xi)\bigg|_{\Xi=0}. \tag{28}$$

If there are two or more statistically independent random variables, e.g. ξ and υ their moment generating function is the product of the moment generating functions for their individual distribution functions $f_\xi(\xi)$ and $f_\upsilon(\upsilon)$:

$$M(\Xi, \Upsilon) = \int_{-\infty}^{\infty}\int_{-\infty}^{\infty} e^{-\Xi\xi-\Upsilon\upsilon} f(\xi,\upsilon) d\xi d\upsilon = \int_{-\infty}^{\infty} e^{-\Xi\xi} f_\xi(\xi) d\xi \int_{-\infty}^{\infty} e^{-\Upsilon\upsilon} f_\upsilon(\upsilon) d\upsilon = M_\xi(\Xi) M_\upsilon(\Upsilon). \tag{29}$$

In general it is not necessarily known what the statistical independent observable quantities are, but we can find them by demanding that their joint moment generating function is the product of their individual moment generating functions. One way to do this is to define the cumulant generating function as the logarithm of of the moment generating function:

$$K(\Xi, \Upsilon) = \ln(M(\Xi, \Upsilon)) = \ln(M_\xi(\Xi)) + \ln(M_\upsilon(\Upsilon)). \tag{30}$$

The cumulants are simply the successive derivatives of the cumulant generating function at $\Xi = 0$ and $\Upsilon = 0$. Cumulants fulfill the definition of statistical independence by construction.

In the framework of the lattice Boltzmann model cumulants can be used for two tasks: First, cumulants make the derivation of the equilibrium state trivial. In equilibrium all non-conserved statistically independent random variables vanish. That is to say, all cumulants other than the conserved ones are zero. In the context of isothermal lattice Boltzmann models that do not conserve kinetic energy, the temperature cumulant is an exception of this rule. Second, if different relaxation rates are assigned to different observable quantities it must be ensured that these quantities are statistically independent. Quantities that are linked through correlation cannot evolve on different time scales. This is the main difference between the cumulant lattice Boltzmann model and the standard multiple relaxation time (MRT) model [18]. In the MRT model no attempts are made to guarantee that the quantities that evolve on different time scales are statistically independent [6]. In contrast, the cumulant lattice Boltzmann model assigns different relaxation rates to different cumulants and achieves a drastic increase in both stability and accuracy over the classical MRT model [6, 19, 20, 21, 22].

In what follows we will refer to the countable cumulants $c_{\alpha\beta\gamma}$ of the distribution f_{ijk} which we define as:

$$c_{\alpha\beta\gamma} = c^{-\alpha\beta\gamma} \frac{\partial^\alpha \partial^\beta \partial^\gamma}{\partial \Xi^\alpha \partial \Upsilon^\beta Z^\gamma} \ln(\mathcal{L}(f_{ijk}))\bigg|_{\Xi=\Upsilon=Z=0}. \tag{31}$$

In practice cumulants are computed from moments by applying the chain rule to Eq. (31) and by comparing to the formal definition of raw moments which can be simplified to the commonly used expression (i.e. Eq. (12)):

$$m_{\alpha\beta\gamma} = c^{-\alpha\beta\gamma} \frac{\partial^\alpha \partial^\beta \partial^\gamma}{\partial \Xi^\alpha \partial \Upsilon^\beta Z^\gamma} \mathcal{L}(f_{ijk})\bigg|_{\Xi=\Upsilon=Z=0} = \sum_{i,j,k} i^\alpha j^\beta k^\gamma f_{ijk}. \tag{32}$$

5. Galilean invariance

Our aim here is to derive lattice Boltzmann models which are fourth order Galilean invariant in diffusive scaling. To this end we should perform the asymptotic expansion of the equivalent partial differential equation for the first moments to fifth order $m^{(5)}_{100}$, $m^{(5)}_{010}$ and $m^{(5)}_{001}$ and interpret the results with regard to reference frame independence. This would be quite involved and we propose a simpler but still sufficient method. It was first proposed in the context of the cascaded lattice Boltzmann model [2, 23, 4] that it is sufficient to chose frame independent variables for the lattice Boltzmann model to obtain Galilean invariance. On a lattice with a finite number of velocities it is only possible to chose a finite number of moments/cumulants to be reference frame independent such that Galilean invariance can only be archived with a finite order of accuracy. Exploiting the structure of the asymptotic analysis (without actually doing it) we can derive sufficient conditions for Galilean invariance at a certain asymptotic order. In particular, for fourth order accuracy we have to evaluate the recursive asymptotic expansion (Eq. (19)) with $\alpha = 1, \beta = 0, \gamma = 0$, and $r = 5$. This incorporates an expansion of the second moments to fourth order, third moments to third order and fourth moments to second order. In addition fifth moments have to be expanded to first order but this has no influence on Galilean invariance as any expansion to first order in diffusive scaling is necessarily linear in velocity. One way of imposing Galilean invariance is to make all observable quantities equivalent to up to fourth order moments statistically independent of velocity within the required asymptotic order. Cumulants are an excellent tool for doing this, since cumulants are by design Galilean invariant.

For a fourth order Galilean invariant lattice Boltzmann scheme we hence demand:

$$c^{eq}_{110},\ c^{eq}_{101},\ c^{eq}_{011},\ c^{eq}_{200} - c^{eq}_{020},\ c^{eq}_{200} - c^{eq}_{002} = O(\epsilon^5), \tag{33}$$

$$c^{eq}_{300},\ c^{eq}_{030},\ c^{eq}_{003},\ c^{eq}_{111},\ c^{eq}_{120},\ c^{eq}_{102},\ c^{eq}_{210},\ c^{eq}_{012},\ c^{eq}_{201},\ c^{eq}_{021} = O(\epsilon^4), \tag{34}$$

$$c^{eq}_{400},\ c^{eq}_{040},\ c^{eq}_{004},\ c^{eq}_{310},\ c^{eq}_{301},\ c^{eq}_{130},\ c^{eq}_{031},\ c^{eq}_{103},\ c^{eq}_{013},\ c^{eq}_{211},\ c^{eq}_{121},\ c^{eq}_{112},\ c^{eq}_{220},\ c^{eq}_{202},\ c^{eq}_{022} = O(\epsilon^3). \tag{35}$$

These are 32 constraints that add to the four or five conserved quantities. It is of note that the fulfillment of all constraints would also guarantee the isotropy of the Galilean invariance to fourth order as cumulants always map on cumulants of the same of the same order under rotation. The easiest way to impose all constraints is to chose a velocity set in which all the above cumulants can be freely adjusted. However, this would involve many discrete velocities considering the fact that no optimal velocity set is known with the properties

- to be a dual of a regular lattice such that it can be implemented in the usual stream and collide fashion of the LBE
- to offer all the required degrees of freedom
- to do this without introducing higher order cumulants which are not required for our purpose but are degrees of freedom of the model.

The direct discretization of all required moments, albeit possible, appears to be unacceptable expensive. We like to point out that the cumulants do not need to be matched exactly by the discretization, it is sufficient if the 15 fourth order cumulants are matched only up to second order in diffusive scaling. Whether this can be done without explicitly discretizing them (i.e. using a much smaller velocity set than the one necessary for the direct discretization) depends on the aliasing properties of the respective velocity set used.

The aliasing properties of a velocity set can be examined by expressing all the individual distributions f_{ijk} in terms of the equivalent low order moments (i.e. by the same number of moments as there are discrete velocities). When other, usually higher, moments of the same discrete distribution are calculated they turn out to be functions of the lower order moments.

Applying the chain rule to the definition of cumulants it is possible to derive explicit equations for cumulants in terms of moments. Taking, for example, the cumulants c_{100}, c_{200}, c_{300} and c_{400} we obtain:

$$
\begin{aligned}
c_{100} &= m_{100}/m_{000}, && (36)\\
c_{200} &= m_{200}/m_{000} - m_{100}^2/m_{000}^2, && (37)\\
c_{300} &= m_{300}/m_{000} - 3m_{100}m_{200}/m_{000}^2 + 2m_{100}^3/m_{000}^3, && (38)\\
c_{400} &= m_{400}/m_{000} - 4m_{100}m_{300}/m_{000}^2 - 3m_{200}^2/m_{000}^2 + 12m_{100}^2m_{200}/m_{000}^3 - 6m_{100}^4/m_{000}^4. && (39)
\end{aligned}
$$

These equations can be solved to express moments in terms of cumulants:

$$
\begin{aligned}
m_{100}/m_{000} &= c_{100}, && (40)\\
m_{200}/m_{000} &= c_{200} + c_{100}^2, && (41)\\
m_{300}/m_{000} &= c_{300} + 3c_{100}c_{200} + c_{100}^3, && (42)\\
m_{400}/m_{000} &= c_{400} + 3c_{200}^2 + 4c_{300}c_{100} + 6c_{200}c_{100}^2 + c_{100}^4. && (43)
\end{aligned}
$$

It is assumed that:

$$
\begin{aligned}
c_{100} &= O(\epsilon), && (44)\\
c_{200} &= \theta + O(\epsilon^2), && (45)\\
c_{300} &= O(\epsilon^3), && (46)\\
c_{400} &= O(\epsilon^4), && (47)
\end{aligned}
$$

where θ is a measure of temperature related to the speed of sound by $c_s = \theta^{1/2}c$. The temperature can be freely chosen in isothermal lattice Boltzmann models (i.e. models without energy conservation). Inserting the cumulants into the aliased equations for moments that are not independent allows us to interpret whether or not a cumulant is sufficiently approximated on a given lattice.

5.1. D3Q27 lattice

We start with a discussion of the Cartesian standard lattice with 27 speeds, that does not support fourth order accurate advection, in order to explain the problem we are facing.

The D3Q27 lattice supports all third order cumulants expect of c_{300}, c_{030} and c_{003} as independent variables. It also supports the fourth order cumulants c_{220}, c_{202}, c_{022}, c_{211}, c_{121} and c_{112} independently. It is hence missing the cumulants c_{400} and c_{310} and all their permutations. Cumulants that are not independently supported take up a value governed by their aliasing structure. Violations of Galilean invariance must originate from the missing cumulants. We hence check for the aliasing of c_{300}:

$$
c_{300} = c_{100}(1 - 3c_{200} - c_{100}^2). \quad (48)
$$

Eq. (48) cannot be further simplified since all terms involved are third order in ϵ. It is, however, possible to replace c_{200} by its equivalent partial differential equation in which ν indicates the kinematic viscosity. However, while Eq. (48) is general and applies to the pre- and the post-collision state of c_{300} the replacement of c_{200} depends on its current state. We write it here in the bared form as this is the form that appears in the asymptotic expansion:

$$
\bar{c}_{300} = c_{100}(1 - 3\theta + 2\nu\partial_x c_{100} - c_{100}^2) + O(\epsilon^4). \quad (49)
$$

It is evident that the leading order of $\bar{c}_{300}$ disappears if and only if $\theta = 1/3$. This is sufficient to obtain second order Galilean invariance but it is insufficient for fourth order Galilean invariance since the remaining terms are of order $O(\epsilon^3)$. It is hence seen that this lattice does not support fourth order accurate Galilean invariance.

To understand the problem better we also check for the unsupported fourth order cumulants. First we compute the aliasing structure of c_{400}:

$$\begin{aligned} c_{400} &= c_{100}^2(6c_{200}-3)+c_{200}(1-3c_{200})+c_{100}^4 \\ &= c_{100}^2(6\theta-3)+c_{200}(1-3\theta)+O(\epsilon^3). \end{aligned} \tag{50}$$

In order to obtain second order accurate Galilean invariance according to Eq. (49) we were required to chose $\theta = 1/3$. We see that this is ineffective for setting c_{400} to $O(\epsilon^3)$. We hence see that also the cumulant c_{400} limits the accuracy of the D3Q27 lattice to second order.

Finally we look at the cumulant c_{310}:

$$\begin{aligned} c_{310} &= c_{010}c_{100}-c_{010}c_{100}^3+c_{110}-3c_{100}^2c_{110}-3c_{010}c_{100}c_{200}-3c_{110}c_{200}-3c_{100}c_{210}-c_{010}c_{300} \\ &= (c_{110}+c_{100}c_{010})(1-3\theta)+O(\epsilon^3). \end{aligned} \tag{51}$$

It is seen that this error vanishes to the required order if $\theta = 1/3$ which is the same condition as for c_{300} to allow second order accuracy.

We can summarize the situation for the D3Q27 lattice as follows. In order to obtain second order accuracy in Galilean invariance the aliasing structure of c_{300} requires us to chose $\theta = 1/3$. With the same value c_{310} is accurate enough to support fourth order Galilean invariance even if we cannot adjust c_{310} and its permutations independently. The cumulant c_{400} is accurate enough to support second order Galilean invariance but it cannot be made to support fourth order Galilean invariance by any choice of θ. We hence see that the reasons why the D3Q27 lattice cannot support fourth order accurate Galilean invariance are linked to the cumulants c_{300} and c_{400} and their permutations alone. It is a very important observation that these two cumulants have no mixed indexes. This implies that they appear only in connection with derivatives of u in direction x. The violations of Galilean invariance appear for flows which are perfectly aligned with the Cardinal directions. At least for the D3Q27 lattice it is therefore sufficient to study the problem with axis aligned flows.

5.2. RD3Q27 lattice

Regarding the body centered cubic lattice with 27 speeds all third order moments are explicitly supported. Also the cumulants of fourth order of the type c_{220} and c_{211} are explicitly supported. Not supported independently of other fourth order cumulants are the cumulants of the type c_{310} and c_{400}. It is however possible to set a combination, namely $m_4 = m_{400} + m_{040} + m_{004}$. We can check now whether this is enough by computing the cumulant c_{400} in terms of other cumulants. For the fourth moment we obtain:

$$m_{400} = \frac{1}{3}(m_4 + m_{000}(-c_{001}^2 - c_{010}^2 + 2c_{100}^2 - c_{002} - c_{020} + c_{200} + m_4)). \tag{52}$$

Inserting this in the cumulant equation gives:

$$c_{400} = \frac{1}{3}(-c_{001}^2 - c_{0101}^2 + 2c_{100}^2 - c_{002} - c_{020} + 2c_{200} - 9c_{200}^2 - 12c_{300}c_{100} - 18c_{200}c_{100}^2 - 3m_{100}^4 + m_4/m_{000}). \tag{53}$$

Eliminating all terms of $O(\epsilon^3)$ reduces this to:

$$c_{400} = \frac{1}{3}(-c_{001}^2 - c_{010}^2 - c_{100}^2 - 9\theta^2 - (18\theta-3)c_{100}^2 + m_4/m_{000}) + O(\epsilon^3). \tag{54}$$

We can choose m_4 freely and we should chose it in such a way that the second order residual vanishes and $c_{400} = O(\epsilon^3)$. However, we have to keep in mind that m_4 also appears in c_{040} and c_{004} such that it has to be invariant under the permutation of the indexes. This is only possible if at the same time $\theta = 1/6$ and:

$$m_4 = \frac{m_{000}}{3}(c_{001}^2 + c_{010}^2 + c_{100}^2 + 1/4) + O(\epsilon^3). \tag{55}$$

It is hence seen that the correct cumulant is only recovered for a specific speed of sound or reference temperature which means that we can either have energy conservation or fourth order Galilean invariance but not both.

In addition we have to check for the cumulant c_{310}:

$$\begin{aligned} c_{310} &= c_{010}c_{100} - 3c_{001}^2c_{010}c_{100} - 3c_{002}c_{010}c_{100} - 6c_{001}c_{011}c_{100} - 3c_{012}c_{100} - c_{010}c_{100}^3 \\ &\quad -6c_{001}c_{010}c_{101} - 6c_{011}c_{101} - 3c_{010}c_{102} + c_{110} - 3c_{001}^2c_{110} - 3c_{002}c_{110} - 3c_{100}^2c_{110} \\ &\quad -6c_{001}c_{111} - 3c_{112} - 3c_{010}c_{100}c_{200} - 3c_{110}c_{200} - 3c_{100}c_{210} - c_{010}c_{300} \\ &= (c_{110} + c_{100}c_{010})(1 - 6\theta) + O(\epsilon^3). \end{aligned} \tag{56}$$

It is seen that also this residual disappears for $\theta = 1/6$. It is therefore possible to obtain fourth order Galilean invariance on the body centered cubic lattice if and only if the reference temperature is $1/6$.

5.3. D3Q33 lattice

On the D3Q33 lattice, the aliasing structure of the cumulant c_{310} is identical to the one on the D3Q27 lattice:

$$c_{310} = (c_{110} + c_{100}c_{010})(1 - 3\theta) + O(\epsilon^3). \tag{57}$$

Since cumulants of the type c_{310} are the only fourth order cumulants on the D3Q33 lattice that are not independent of others we see that it is only required to set $\theta = 1/3$ to recover fourth order Galilean invariance. Again, fourth order Galilean invariance is only possible on this lattice if the temperature is constant (i.e. without energy conservation).

5.4. Implications of the optimality condition

We identified that $\theta = 1/6$ is a necessary condition for fourth order Galilean invariance on the body centered cubic RD3Q27 lattice. It is interesting to note in this regard that this is not the value chosen by Namburi et al. in their original paper [8]. Instead they chose $\theta = 1/5$ as the reference value for isothermal simulations. Unfortunately, they had a good reason to take this suboptimal value. In the context of the BGK lattice Boltzmann equation [24], which is typically not derived from cumulants, the value of the distribution function in equilibrium at zero velocity and unit mass is called the weight of the velocity. The body centered cubic lattice has four energy shells for the different weights that take the values $w_{000} = 1/3$, $w_{100} = 1/30$, $w_{110} = 1/300$ and $w_{\frac{1}{2}\frac{1}{2}\frac{1}{2}} = 4/75$ for $\theta = 1/5$. If we chose instead $\theta = 1/6$ these weights change to $w_{000} = 7/18$, $w_{100} = 1/36$, $w_{110} = 0$ and $w_{\frac{1}{2}\frac{1}{2}\frac{1}{2}} = 1/18$. The weight for the 12 diagonal directions (w_{110}) vanishes. In the context of the BGK collision operator a vanishing weight for any direction would imply that the distribution moving with the respective velocity would always be zero. In case of the cumulant collision operator this is not necessarily so but here it means that the distribution fluctuates around zero, i.e. that the distribution is not a positive function. According to an orthodox interpretation of the momentum distribution function as a probability density negative distributions make no sense. On the other hand, it is instructive to remember that the positivity of the distributions was nowhere used in the derivation of the lattice Boltzmann method and that the only things that require a physical interpretation are the governing equations for the conserved quantities. That some of the distributions might be zero or negative is not wrong per se as long as the correct equations are being solved. Nevertheless, having non-positive distributions might imply some problems.

Interestingly, the D3Q33 has the same problem. The weights for the distributions going to next-next-neighbors w_{200} is zero for the required temperature $\theta = 1/3$. However, in this case the problem is less severe as there are still 27 non-zero weights. On the body centered cubic lattice there are only 15 non-zero weights for the required temperature.

6. D3Q27F3 model

In addition to the monolithic lattice Boltzmann models on the RD3Q27 and the D3Q33 lattices we propose here a hybrid modification of the standard D3Q27 lattice which we supplement by three finite differences (D3Q27F3 lattice). In order to derive the necessary modifications to the standard D3Q27 model for fourth order Galilean invariance we expand Eq. (19) for $\alpha = 1, \beta = 0$ and $\gamma = 0$. For clarity we drop the derivatives in y and z as they do not contribute to problem under investigation:

$$0 = -\partial_t \bar{m}_{100} - \partial_x \bar{m}_{200} + \frac{1}{12}\partial_{xxx}\bar{m}_{400} \cdots \tag{58}$$

On the D3Q27 lattice the cumulants c_{300} and c_{400} are not independent of lower order cumulants as shown in Eq. (48) and Eq. (50).

In the following we denote by $u = c_{100}$, $v = c_{010}$ and $w = c_{001}$ the velocity components in x, y and z direction, respectively. The density is $\rho = m_{000}$.

Due to the incorrect cumulants $\bar{m}_{300}$ and $\bar{m}_{400}$ are misrepresented on the D3Q27 lattice. Specifically $\bar{m}_{400}$ misses a term ρu^2. In addition, when we expand Eq. (19) for $\alpha = 2, \beta = 0$ and $\gamma = 0$ we find that due to the error in Eq. (49) $\bar{m}_{200}$ is missing a term $-3\nu(3u^2\partial_x u - 6\nu\partial_x(u\partial_x u))$. Inserting all of this into the expanded equation for momentum gives us a term A which is the term that distinguishes the equation solved by the D3Q27 cumulant method without correction from the Navier-Stokes equation:

$$A = -\partial_x(-3\rho\nu(3u^2\partial_x u - 6\nu\partial_x(u\partial_x u))) + \frac{1}{12}\partial_{xxx}(\rho u^2). \tag{59}$$

Which can be rewritten as:

$$A = -\partial_x[-3\nu\rho(3u^2\partial_x u) + \rho(18\nu^2 - \frac{1}{6})((\partial_x u)(\partial_x u) + u\partial_{xx}u)]. \tag{60}$$

This can be implemented in the lattice Boltzmann method by modifying the equilibrium of the second cumulant c_{200} to be:

$$c_{200}^{eqMOD} = c_{200}^{eq} + (-3\nu(3u^2\partial_x u) + (18\nu^2 - \frac{1}{6})((\partial_x u)(\partial_x u) + u\partial_{xx}u)). \tag{61}$$

Using this modified equilibrium for the second order cumulants permits fourth order Galilean invariance even on a standard lattice. However, in order to implement the modified equilibrium two kinds of spatial derivatives have to be computed, namely $\partial_x u$ and $\partial_{xx} u$. The first derivative $\partial_x u$ is easily computed from the second order cumulants and including the first correction is already standard [6, 25]. Including the terms proportional to $\partial_{xx} u$ requires more work since no efficient way to compute the second derivative locally from the cumulants has yet been found. Therefore, we will use finite differences to compute $\partial_{xx} u$, $\partial_{yy} v$ and $\partial_{zz} w$.

In order to exploit the existing data structure of the lattice Boltzmann kernel we implement the computation of the second derivatives in a slightly unusual way. We use the fact that the first derivative of velocity $\partial_x u$ is known on each lattice node at collision time. It is computed from:

$$\partial_x u \approx -\frac{3}{2}\omega_1(c_{200} - \theta), \tag{62}$$

with ω_1 being the relaxation rate of the second cumulants related to shear (see [6] for more detail). Instead of querying neighboring nodes for their velocity we pack the value of $\partial_x u$ into a new distribution and send it together with the outgoing distribution to the neighbors in positive and negative x direction, i.e.:

$$\begin{aligned}
g_{100(x+\Delta x)yz(t+\Delta t)} &= \partial_x u|_{xyzt}\,, && (63)\\
g_{\bar{1}00(x-\Delta x)yz(t+\Delta t)} &= \partial_x u|_{xyzt}\,, && (64)\\
g_{010x(y+\Delta x)z(t+\Delta t)} &= \partial_y v\big|_{xyzt}\,, && (65)\\
g_{0\bar{1}0x(y-\Delta x)z(t+\Delta t)} &= \partial_y v\big|_{xyzt}\,, && (66)\\
g_{001xy(z+\Delta x)(t+\Delta t)} &= \partial_z w|_{xyzt}\,, && (67)\\
g_{00\bar{1}xy(z-\Delta x)(t+\Delta t)} &= \partial_z w|_{xyzt}\,. && (68)
\end{aligned}$$

The second derivative can be approximated in the next time step by:

$$\partial_{xx} u \approx \frac{g_{\bar{1}00xyzt} - g_{100xyzt}}{2}. \tag{69}$$

It should be noted that, compared to the usual method of computing a finite difference, this finite difference has a time delay. But asymptotic considerations imply that the delay is irrelevant (i.e. in order to impose fourth order

Galilean invariance the correction needs only second order accuracy). The advantage of the method proposed here is that the finite difference shares the stream and collide algorithm with the LBM. That is to say, no additional algorithmic step is introduced. On top of this, the proposed method introduces six new variables, the same number as going from the D3Q27 to the D3Q33 lattice. However, while the D3Q33 method has to address next-next-nearest neighbors, the D3Q27F3 method uses only the standard neighborhood of the D3Q27 lattice. The D3Q27F3 method is hence algorithmically at least as efficient as the D3Q33 method. The stencil is shown in Fig. 2.

7. Implementation

All proposed models are implemented with cumulant collision operator as described in detail in [6]. First, central moments are computed from the distributions $f_{ijkzyxzt}$. The central moments are then transformed into cumulants and each cumulant relaxes with its own rate to the equilibrium. For simplicity we distinguish here only two different relaxation rates. The rate ω_1 relaxing the cumulants related to shear (i.e. $c_{200} - c_{020}$, $c_{200} - c_{002}$, c_{110}, c_{101} and c_{011}) and the rate $\omega_r = 1$ for all remaining non-conserved cumulants. We note here that this is not the optimal choice for diffusion [26] but it is sufficient if we are concerned only about Galilean invariance. The kinematic viscosity is computed from:

$$\nu = c_s^2\left(\frac{1}{\omega_1} - \frac{1}{2}\right). \tag{70}$$

The equilibria for all non-conserved cumulants is zero. The only exception is the energy cumulant $c_{200}+c_{020}+c_{002}$ which is not a conserved quantity in isothermal lattice Boltzmann models. Its equilibrium is:

$$c_{200}^{eq} + c_{020}^{eq} + c_{002}^{eq} = 3\theta. \tag{71}$$

The reference temperature is hence defined by setting the equilibrium of the energy cumulant.

Since the relaxation rates of all cumulants beyond the second cumulants is set to one all the higher cumulants which are independent quantities are set to zero in the collision. This means in particular that all third order cumulants on the RD3Q27 and D3Q33 lattices are set to zero. Also all available fourth order cumulants are set to zero. On the RD3Q27 lattice the moment m_4 given in Eq. (55) is an additional constraint due to the fact that the cumulants c_{400}, c_{040}, and c_{004} cannot be set individually.

The D3Q27F3 method is implemented as in [6] with the equilibria for the second order cumulants replaced by:

$$c_{200}^{eq} = \theta + (-3\nu\rho(3u^2\partial_x u) + \rho(18\nu^2 - \frac{1}{6})((\partial_x u)(\partial_x u) + u\partial_{xx}u)), \tag{72}$$

$$c_{020}^{eq} = \theta + (-3\nu\rho(3v^2\partial_y v) + \rho(18\nu^2 - \frac{1}{6})((\partial_y v)(\partial_y v) + v\partial_{yy}v)), \tag{73}$$

$$c_{002}^{eq} = \theta + (-3\nu\rho(3w^2\partial_z w) + \rho(18\nu^2 - \frac{1}{6})((\partial_z w)(\partial_z w) + w\partial_{zz}w)). \tag{74}$$

For simplicity we neglected the bulk viscosity in the derivation of Eq. (72)-(74). All simulations below are conducted with this form of the correction. The correction terms can also be derived under consideration of the bulk viscosity, but then they cannot be written easily in terms of equilibria as in Eq. (72)-(74). The modified collision operator for second order cumulants incorporating an independent bulk viscosity is given in Appendix A.

Finally we note that the collision operator for the cumulant c_{400} and its permutation on the D3Q33 was implemented in raw moment space by computing the post-collision raw moment m_{400}^* from the post-collision second order moment m_{200}^*:

$$m_{400}^* = m_{200} + \rho u^2. \tag{75}$$

This implements the correct cumulant to the required asymptotic order.

8. Numerical tests

In [6] we argued that the cumulant lattice Boltzmann model on the standard D3Q27 removes most artifacts in Galilean invariance. For example, it removes the velocity dependence of viscosity from the lattice Boltzmann equation. Also the phase shift in a traveling decaying shear wave was found to be fourth order accurate. However, due to the absence of some third and fourth order cumulants we observed a phase lag in the advection of a traveling Taylor-Green vortex which could not be removed. Even though the method is still second order accurate, we found that the phase error is essentially independent of the magnitude of the velocity at fixed Reynolds number. Hence the error can only be reduced by refining the grid, which is very expensive. After removing all other leading errors from the advection, this phase lag is the dominant and hence most painful error. With the three proposed new methods it is possible to eliminate this phase lag. We demonstrate this below by simulating the traveling Taylor-Green vortex. In addition we simulate a traveling double shear wave. In both cases the background velocity is aligned with a grid axis. This is done here mainly for practical reasons as the phase lag can be more easily measured if the flow returns to its original position. Note that, the original D3Q27 cumulant model already removed all leading errors in Galilean invariance up to the ones where the velocity and the derivative directions are aligned with the same Cardinal lattice directions. We will hence probe Galilean invariance with respect to flow along the Cardinal directions.

For all test cases below it should be kept in mind that, due to the BCC lattice structure, the RD3Q27 simulations contain twice as many nodes as the D3Q27 and D3Q33 simulations at the same resolution.

8.1. Traveling Taylor-Green vortex

The numerical setup for the decaying Taylor-Green vortex is taken from [6]. We initialize a vortex on a plain rectangular domain. The initial conditions are:

$$\begin{aligned} u(0) &= u_0 L_0/L + U L_0/L \sin(2\pi x/L)\cos(4\pi z/(3L)), \\ v(0) &= 0, \\ w(0) &= -3/2 U L_0/L \cos(2\pi x/L)\sin(4\pi z/(3L)), \\ \rho(0) &= \left(1 - \frac{3U^2 L_0^2}{16L^2}(9\cos(4\pi x/L) + 4\cos(8\pi z/(3L)))\right). \end{aligned} \tag{76}$$

The reference length is $L_0 = 32\Delta x$ and the grid length L is varied from $32\Delta x$ to $128\Delta x$ to measure the asymptotic behavior of the phase shift. Two different velocities are used: a fast set with $U = 0.00390625\Delta x/\Delta t$ and $u_0 = 0.1\Delta x/\Delta t$ and a slow velocity with $U = 0.000390625\Delta x/\Delta t$ and $u_0 = 0.01\Delta x/\Delta t$. By varying L the velocity amplitude and advection velocity in Eq. (76) is scaled. The test case hence uses diffusive scaling.

We test five different models: the original cumulant lattice Boltzmann model on the D3Q27 lattice, the cumulant lattice Boltzmann model on the D3Q33 lattice, the hybrid cumulant lattice Boltzmann model on the D3Q27F3 lattice, and the cumulant lattice Boltzmann model on a body centered cubic lattice RD3Q27 with $\theta = 1/5$ and $\theta = 1/6$.

The advection velocity is chosen such that the vortex should return to its initial position after time $L^2/(L_0 u_0)$. We call this time the overflow period. By taking a Fourier transform of the velocity field at discrete time steps separated by the overflow period and selecting the wave number of the vortex we can measure the phase lag $\Delta\phi$ of the vortex. To improve the accuracy of the measurement and allow the initial transient to die out we use linear regression of the fifth to eight overflow periods. In the high velocity case it was observed by looking at the time series that the initial transient had not disappeared after five turnovers such that the measurement window was shifted to a later time. The results are reported in Fig. 3 for the high advection velocity and in Fig. 4 for the low velocity.

In agreement with our predictions, the D3Q27 and the $\text{RD3Q27}_{1/5}$ model with $\theta = 1/5$ show strictly second order convergence while all other models show fourth order convergence for the phase shift of the traveling Taylor-Green vortex. The fourth order convergence is more clearly seen in the low velocity case than in the high velocity case which is in accordance with asymptotic theory. While the $\text{RD3Q27}_{1/6}$ ($\theta = 1/6$) model gives the lowest phase shift of all models at the highest viscosity for the low advection velocity, the method is found to be stable only for viscosity $\nu = 10^{-2}\Delta x^2/\Delta t$. In all other cases the method crashed. It is interesting to see that the hybrid D3Q27F3 method is slightly more accurate than the monolithic D3Q33 method. Both methods share the same number of degrees of freedom but the stencil of the D3Q27F3 method is more compact as seen in Fig. 2.

As for the second order accurate methods, it is of note that the RD3Q27$_{1/5}$ model with the reference temperature proposed by Namburi et al. [8] is stable and has a noticeable lower phase error than the Cartesian D3Q27 method.

One important observation from the comparison of the phase lag in the high (Fig. 3) and low (Fig. 4) velocity case is that there is no significant difference in the phase error between different velocities. This implies that the phase error cannot be reduced by choosing a smaller Mach number or, equivalently, by choosing a shorter time step. Making the time step shorter reduces the accumulation of errors by the same amount as it increases the number of time steps required to reach a given physical time. The error can be reduced by spending more resolution in space but it cannot be removed by spending more resolution in time. This makes the phase error a numerically very expensive error which also justifies the introduction of more degrees of freedom in order to remove it.

8.2. Double shear wave

As for the second order accurate methods, in the last section the RD3Q27$_{1/5}$ method appears to show a considerable improvement over the standard D3Q27 method. This is even true if we take into account that the computational cost of the RD3Q27 simulations are twice as high as for the D3Q27 simulations at the same resolution. However, the apparent superiority of the the RD3Q27$_{1/5}$ method is due to the considered test case and we add here another test in order to show that this might be misleading. In [6] we showed that the standard cumulant lattice Boltzmann method on a Cartesian grid obtains fourth order accuracy for axis alined traveling double shear waves. The setup is very similar to that of the planar traveling Taylor-Green vortex. The initial conditions are given by:

$$\begin{aligned} u(0) &= u_0 L_0/L, \\ v(0) &= V L_0/L \sin(2\pi x/L) \sin(4\pi z/(3L)), \\ w(0) &= 0, \\ \rho(0) &= 1. \end{aligned} \tag{77}$$

Here V is the amplitude of the wave and it takes the same values as U in the case of the traveling Taylor-Green vortex test. The measurement principle of the phase delay $\Delta\phi$ per overflow period is the same as in the previous example. Results are shown in Fig. 5 (fast) and Fig. 6 (slow). The cumulant lattice Boltzmann method on Cartesian grids does not require any corrections to obtain fourth order accuracy in that case. This is seen from the fact that all terms of the type $u\partial_{xx}u$ are zero in the case of the double shear wave. It is hence expected that the D3Q27, the D3Q33 and the D3Q27F3 show basically identical results in regard of phase shift. This is also confirmed by the results of Fig. 5 and Fig. 6. However, for the D3Q33 we observe the expected behavior only at high enough viscosity. The D3Q33 method becomes unstable for viscosity $\nu = 10^{-3}\Delta x^2/\Delta t$ and smaller. The D3Q27F3 method remains stable in the entire measurement range.

There is also a significant difference between the results for the RD3Q27$_{1/5}$ and the RD3Q27$_{1/6}$ method. Only with the optimized temperature is the advection of the body centered cubic method fourth order accurate. With the reference temperature proposed by Namburi et al. [8] the phase lag of the traveling shear wave test case is very similar to the one measured with the Taylor-Green vortex test. This behavior is explained through Eq. (56). The fourth order cumulant c_{310} is only sufficiently Galilean invariant for $\theta = 1/6$. This is due to the aliasing structure of the RD3Q27 lattice that does not support c_{310} as an independent degree of freedom. A similar condition holds for the D3Q27 and the D3Q33 models with Eq. (51) where θ must be $1/3$ in order to obtain the asymptotically correct value for c_{310}. Fortunately for these Cartesian models, the standard value of θ is already $\theta = 1/3$ such that the cumulant c_{310} turns out to be correct by default.

Everything would be fine for the body centered cubic lattice if the model was sufficiently stable for $\theta = 1/6$, but unfortunately, this does not seem to be the case. Also for the double shear wave test, the RD3Q27$_{1/6}$ method is only stable for viscosities too high to be of practical interest.

9. Conclusions

The phase lag in the advection of vortexes in the cumulant lattice Boltzmann model on Cartesian grids is one of its dominant remaining defects. Albeit it is important to note that drastically more severe defects exist in the majority of

all lattice Boltzmann models that relay on Taylor expanded equilibrium distribution functions instead of cumulants, for extending the lattice Boltzmann model to fourth order accuracy the phase lag is a significant obstacle. This study was originally inspired by our hope that the increased isotropy of the body centered cubic lattice would offer an inexpensive solution to the phase lag problem. While our study showed that this is in principle true and fourth order accuracy of the advection can be obtained with the RD3Q27 lattice, it turned out that this was only possible under unfavorable conditions. Fourth order accuracy of the advection is obtained if and only if the reference temperature is fixed to $\theta = 1/6$ which completely depletes the populations from one of the energy shells. The respective distributions fluctuate around zero and this is found to decrease the stability range of the model in an unacceptable manner. One might say that even though the body centered cubic model succeeded in a theoretical way it failed in a practical way.

As alternatives to the body centered cubic model we proposed two models on Cartesian grids that solve the phase shift problem by using more degrees of freedom. Each of the two models added six populations to the original D3Q27 model such that they have comparable computational cost. The monolithic D3Q33 model suffers from a similar illness as the RD3Q27 model as the application of the reference temperature required for fourth order accuracy depletes an energy shell. While the D3Q33 method has better stability properties than the RD3Q27 model with $\theta = 1/6$ it still suffers from instability in the shear wave example.

It is quite interesting that the hybrid model that repairs the defects of the original D3Q27 lattice through finite differences showed slightly better results in terms of phase lag than the D3Q33 model. From the proposed models, only the D3Q27F3 model showed satisfactory results with respect to stability. It is also important to note that, among all tested models, the D3Q27F3 model is the only one that can easily be reduced to the D3Q27 by a limiter without interfering with conservation laws. That is to say, the corrections involving second derivatives in the D3Q27F3 method could be set to zero in harsh conditions where they might impose a stability risk. Albeit we do not investigate this point in the current paper, it appears to us that controlability of the correction might be an advantage when the method is applied to complex engineering problems.

In addition to the practical result of obtaining several lattice Boltzmann models with fourth order Galilean invariance, the current study is also a success of the theory of cumulants in the context of lattice Boltzmann modeling. As we pointed out, a rigorous derivation of fourth order accuracy requires an asymptotic expansion of the lattice Boltzmann equation up to at least fifth order in diffusive scaling. Such an expansion would be extremely tedious and the results would be difficult to interpret. Cumulants offer a drastic shortcut in the derivation as shown in this paper. We used only the structure of the expansion to determine to which order in diffusive scaling the cumulants of the successive orders have to be matched in order to obtain a given level of accuracy. With this knowledge we could simply propose that a method setting the countable cumulants up to the determined order to zero must result in the prescribed order of Galilean invariance. This we find confirmed in our numerical tests.

The current study is limited to accuracy of the advection. Albeit it was not used here, we found also a way to improve the diffusion to fourth order accuracy. Results on this have been published elsewhere [26, 27].

Acknowledgments

This work was financed by the TU-Braunschweig.

Appendix A. D3Q27F3 with consideration of bulk viscosity

Eq. (72)-(74) are derived under neglect of the bulk viscosity for simplicity. In order to take the bulk viscosity into account we have to consider the actual collision operator, which is listed in Section 4 of [6]. Note that there the collision operator is written in terms of cumulants times density. We define:

$$C_{abc} = \rho c_{abc}. \tag{A.1}$$

Further as detailed in [6], the shear viscosity is adjusted through ω_1 and the bulk viscosity is adjusted through ω_2. In order to incorporate the correction terms under consideration of the bulk viscosity into the standard cumulant method the reader is advised to start from the method given in section 4 of [6] and there to replace Eq. (61)-(63) by the following corrected form:

$$
\begin{aligned}
C^*_{200} - C^*_{020} &= (1-\omega_1)(C_{200} - C_{020}) - 3\rho\left(1 - \frac{\omega_1}{2}\right)(u^2\partial_x u - v^2\partial_y v) \\
&\quad +\rho\omega_1\left(2\left(\frac{1}{\omega_1} - \frac{1}{2}\right)^2 - \frac{1}{6}\right)((\partial_x u)^2 + u\partial_{xx}u - (\partial_y v)^2 - v\partial_{yy}v), \qquad \text{(A.2)} \\
C^*_{200} - C^*_{002} &= (1-\omega_1)(C_{200} - C_{002}) - 3\rho\left(1 - \frac{\omega_1}{2}\right)(u^2\partial_x u - w^2\partial_z w) \\
&\quad +\rho\omega_1\left(2\left(\frac{1}{\omega_1} - \frac{1}{2}\right)^2 - \frac{1}{6}\right)((\partial_x u)^2 + u\partial_{xx}u - (\partial_z w)^2 - w\partial_{zz}w), \qquad \text{(A.3)} \\
C^*_{200} + C^*_{020} + C^*_{002} &= \kappa_{000}\omega_2 + (1-\omega_2)(C_{200} + C_{020} + C_{002}) \\
&\quad -3\rho\left(1 - \frac{\omega_2}{2}\right)(u^2\partial_x u + v^2\partial_y v + w^2\partial_z w) \\
&\quad +\rho\frac{6 - 3(\omega_1+\omega_2) + \omega_1\omega_2}{3\omega_1}((\partial_x u)^2 + u\partial_{xx}u + (\partial_y v)^2 + v\partial_{yy}v + (\partial_z w)^2 + w\partial_{zz}w). \qquad \text{(A.4)}
\end{aligned}
$$

References

[1] P. Lallemand, L.-S. Luo, Theory of the lattice Boltzmann method: dispersion, dissipation, isotropy, Galilean invariance, and stability, Physical review. E, Statistical physics, plasmas, fluids, and related interdisciplinary topics 61 (6 Pt A) (2000) 6546–62.

[2] M. Geier, A. Greiner, J. Korvink, Cascaded digital lattice boltzmann automata for high reynolds number flow, Physical Review E - Statistical, Nonlinear, and Soft Matter Physics 73 (6), cited By 62. doi:10.1103/PhysRevE.73.066705.

[3] M. Geier, A. Greiner, J. Korvink, Galilean invariant viscosity term for an athermal integer lattice boltzmann automaton in three dimensions, Vol. 1, 2004, pp. 255–258.

[4] M. Geier, A. Greiner, J. Korvink, Properties of the cascaded lattice boltzmann automaton, International Journal of Modern Physics C 18 (4) (2007) 455–462. doi:10.1142/S0129183107010681.

[5] M. Geier, A. Greiner, J. Korvink, A factorized central moment lattice boltzmann method, European Physical Journal: Special Topics 171 (1) (2009) 55–61, cited By 17. doi:10.1140/epjst/e2009-01011-1.

[6] M. Geier, M. Schönherr, A. Pasquali, M. Krafczyk, The cumulant lattice boltzmann equation in three dimensions: Theory and validation, Computers & Mathematics with Applications 70 (4) (2015) 507 – 547. doi:http://dx.doi.org/10.1016/j.camwa.2015.05.001.

[7] M. Geier, A. Fakhari, T. Lee, Conservative phase-field lattice boltzmann model for interface tracking equation, Physical Review E - Statistical, Nonlinear, and Soft Matter Physics 91 (6). doi:10.1103/PhysRevE.91.063309.

[8] M. Namburi, S. Krithivasan, S. Ansumali, Crystallographic lattice boltzmann method, Scientific reports 6.

[9] A. Bravais, L. É. de Beaumont, Etudes cristallographiques: Mémoire sur les systèmes formés par des points distribués régulièrement sur un plan ou dans l'espace, Gauthiers-Villars, 1866.

[10] D. dHumières, M. Bouzidi, P. Lallemand, Thirteen-velocity three-dimensional lattice boltzmann model, Physical Review E 63 (6) (2001) 066702.

[11] J. Tölke, M. Krafczyk, Teraflop computing on a desktop pc with gpus for 3d cfd, International Journal of Computational Fluid Dynamics 22 (7) (2008) 443–456.

[12] K. Petkov, F. Qiu, Z. Fan, A. E. Kaufman, K. Mueller, Efficient lbm visual simulation on face-centered cubic lattices, IEEE transactions on visualization and computer graphics 15 (5) (2009) 802–814.

[13] M. Junk, A. Klar, L.-S. Luo, Asymptotic analysis of the lattice Boltzmann equation, J. Comput. Phys. 210 (2) (2005) 676–704. doi:10.1016/j.jcp.2005.05.003.

[14] X. He, X. Shan, G. D. Doolen, Discrete boltzmann equation model for nonideal gases, Phys. Rev. E 57 (1998) R13–R16. doi:10.1103/PhysRevE.57.R13.

[15] P. J. Dellar, An interpretation and derivation of the lattice boltzmann method using strang splitting, Computers & Mathematics with Applications 65 (2) (2013) 129 – 141, special Issue on Mesoscopic Methods in Engineering and Science (ICMMES-2010, Edmonton, Canada). doi:http://dx.doi.org/10.1016/j.camwa.2011.08.047.
URL http://www.sciencedirect.com/science/article/pii/S0898122111007206

[16] F. Dubois, Equivalent partial differential equations of a lattice Boltzmann scheme, Computers & Mathematics with Applications 55 (7) (2008) 1441–1449.

[17] D. J. Holdych, D. R. Noble, J. G. Georgiadis, R. O. Buckius, Truncation error analysis of lattice boltzmann methods, Journal of Computational Physics 193 (2) (2004) 595–619.

[18] D. d'Humières, I. Ginzburg, M. Krafczyk, P. Lallemand, L.-S. Luo, Multiple-relaxation-time lattice Boltzmann models in three dimensions, Phil. Trans. R. Soc. A 360 (2002) 437–451.

[19] M. Krafczyk, K. Kucher, Y. Wang, M. Geier, DNS/LES studies of turbulent flows based on the cumulant lattice boltzmann approach, 2015.

[20] E. K. Far, M. Geier, K. Kutscher, M. Krafczyk, Distributed cumulant lattice boltzmann simulation of the dispersion process of ceramic agglomerates, J. Comput. Meth. in Science and Engineering 16 (2016) 231–252.

[21] E. Far, M. Geier, K. Kutscher, M. Krafczyk, Simulation of micro aggregate breakage in turbulent flows by the cumulant lattice boltzmann method, Computers and Fluids 140 (2016) 222–231, cited By 0. doi:10.1016/j.compfluid.2016.10.001.

[22] A. Pasquali, M. Schönherr, M. Geier, M. Krafczyk, Simulation of external aerodynamics of the drivaer model with the lbm on gpgpus, Parallel Computing: On the Road to Exascale (2016) 391–400.
[23] M. Geier, De-aliasing and stabilization formalism of the cascaded lattice boltzmann automaton for under-resolved high reynolds number flow, International Journal for Numerical Methods in Fluids 56 (8) (2008) 1249–1254. doi:10.1002/fld.1634.
[24] Y. H. Qian, D. d'Humières, P. Lallemand, Lattice BGK models for Navier-Stokes equation, EPL (Europhysics Letters) 17 (6) (1992) 479.
[25] P. J. Dellar, Lattice Boltzmann algorithms without cubic defects in Galilean invariance on standard lattices, Journal of Computational Physics 259 (0) (2014) 270 – 283. doi:http://dx.doi.org/10.1016/j.jcp.2013.11.021.
[26] M. Geier, A. Pasquali, M. Schönherr, Parametrization of the cumulant lattice boltzmann method for fourth order accurate diffusion part i: Derivation and validation, Journal of Computational Physics (2017) –doi:https://doi.org/10.1016/j.jcp.2017.05.040.
URL http://www.sciencedirect.com/science/article/pii/S0021999117304230
[27] M. Geier, A. Pasquali, M. Schönherr, Parametrization of the cumulant lattice boltzmann method for fourth order accurate diffusion part ii: Application to flow around a sphere at drag crisis, Journal of Computational Physics (2017) –doi:https://doi.org/10.1016/j.jcp.2017.07.004.
URL http://www.sciencedirect.com/science/article/pii/S0021999117305065

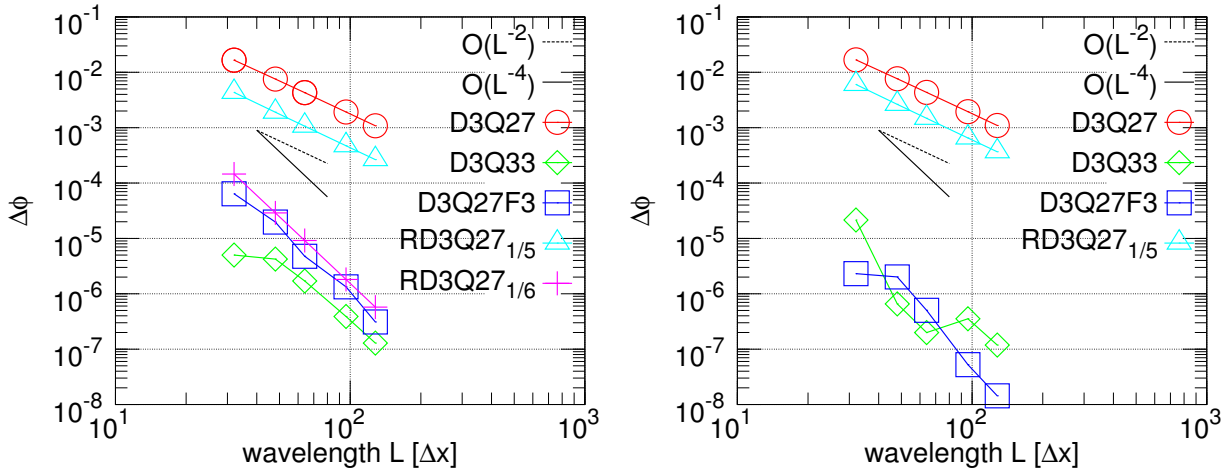

(a) $\nu = 10^{-2}\Delta x^2/\Delta t$ (b) $\nu = 10^{-3}\Delta x^2/\Delta t$

(c) $\nu = 10^{-4}\Delta x^2/\Delta t$ (d) $\nu = 10^{-5}\Delta x^2/\Delta t$

Figure 3: Phase error $\Delta\phi$ for the traveling Taylor-Green vortex with advection velocity $u = 0.1\Delta x/\Delta t L_0/L$. The domain length is $L = \{32, 48, 64, 96, 128\}\Delta x$. The phase error is the difference in phase measured in radiant acquired after one turnover circle. The different sub figures show four different viscosities. Due to the different arrangement of nodes on the RD3Q27 lattice compared to the D3Q27 lattice, all simulations on the RD3Q27 lattice contain twice as many points as the D3Q27 and the D3Q33 lattice at the same resolution. This should be taken into account when comparing the errors. It is seen that the Cartesian D3Q27 and the body centered cubic $\text{RD3Q27}_{1/5}$ with $\theta = 1/5$ are only second order accurate while the other models obtain fourth order accuracy. The $\text{RD3Q27}_{1/6}$ method is stable only for the viscosity $\nu = 10^{-2}\Delta x^2/\Delta t$. It crashed for all other cases. In general, the error appears not to be a strong function of viscosity. The kink of the results for D3Q33 in sub figure (b) is due to a change of sign in the error between $L = 48\Delta x$ and $L = 64\Delta x$.

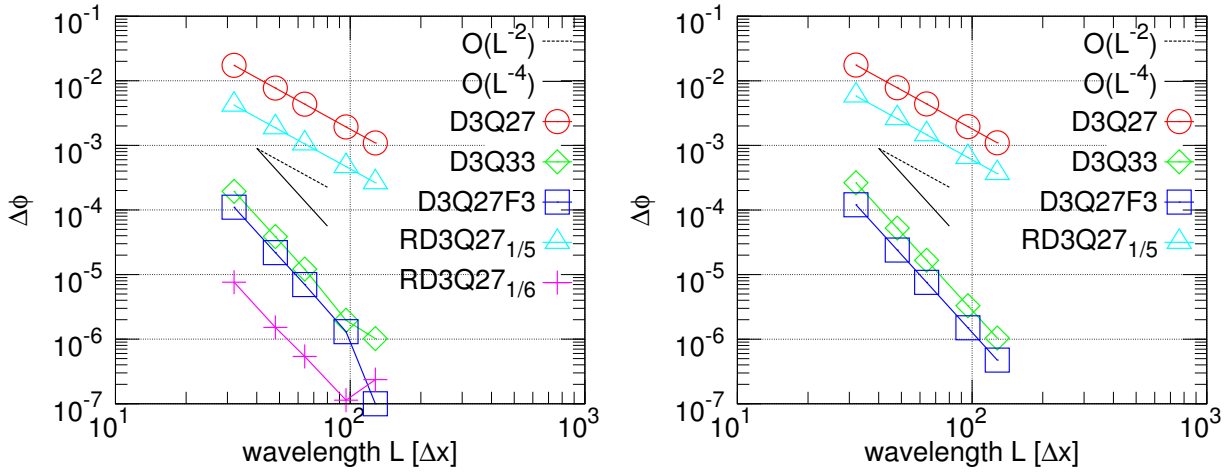

(a) $\nu = 10^{-2}\Delta x^2/\Delta t$ (b) $\nu = 10^{-3}\Delta x^2/\Delta t$

(c) $\nu = 10^{-4}\Delta x^2/\Delta t$ (d) $\nu = 10^{-5}\Delta x^2/\Delta t$

Figure 4: Phase error for the traveling Taylor-Green vortex as in Fig. 3 but with advection velocity $u = 0.01\Delta x/\Delta t L_0/L$. By comparing with Fig. 3 it becomes obvious that the error is almost independent from the advection velocity for the second order accurate models. Note that a ten times smaller advection velocity also means that the turn around time contains ten times more time steps. The fourth order accurate models follow the theory more closely for the small velocity than for the high velocity while there is no drastic difference in the magnitude of the errors between the different velocities. The RD3Q27$_{1/6}$ is again only stable for the highest viscosity. Lowering the velocity does not seem to improve its stability in this case. The kink in the result for RD3Q27$_{1/6}$ in sub figure (a) is due to a change in sign of the error between $L = 96\Delta x$ and $L = 128\Delta x$.

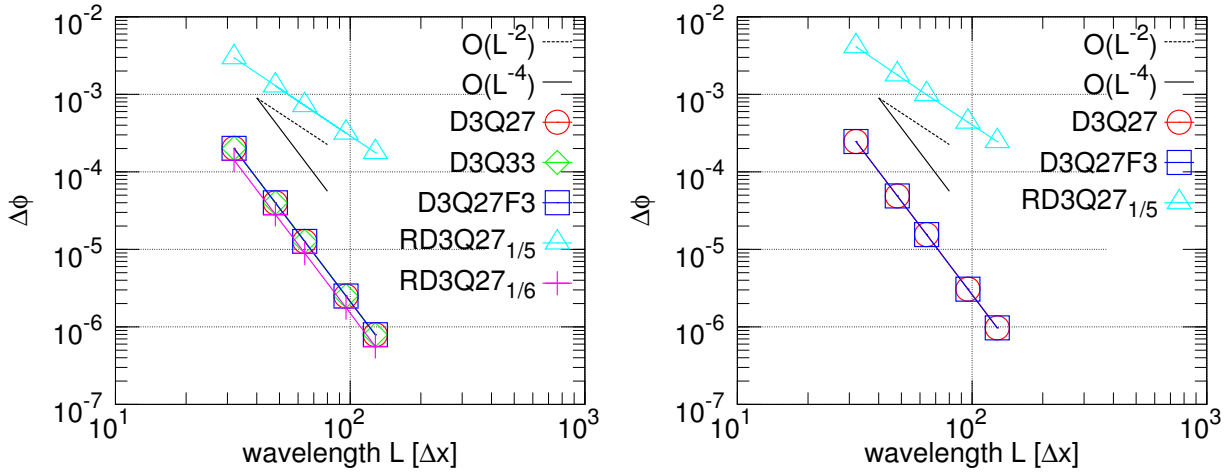

(a) $\nu = 10^{-2}\Delta x^2/\Delta t$ (b) $\nu = 10^{-3}\Delta x^2/\Delta t$

(c) $\nu = 10^{-4}\Delta x^2/\Delta t$ (d) $\nu = 10^{-5}\Delta x^2/\Delta t$

Figure 5: Phase error for the traveling double shear wave with advection velocity $u = 0.1\Delta x/\Delta t L_0/L$. It is seen that even the Cartesian D3Q27 cumulant method is fourth order accurate in this case. The $\text{RD3Q27}_{1/5}$ is only second order accurate with the magnitude of the error being very similar to the phase shift in the Taylor-Green vortex case. Again, the $\text{RD3Q27}_{1/6}$ is fourth order accurate for the highest viscosity but unstable for the three lower viscosities. The D3Q33 shows mixed results. At the highest viscosity it behaves almost identical to the D3Q27 and D3Q27F3 method but it becomes unstable for the lower viscosities.

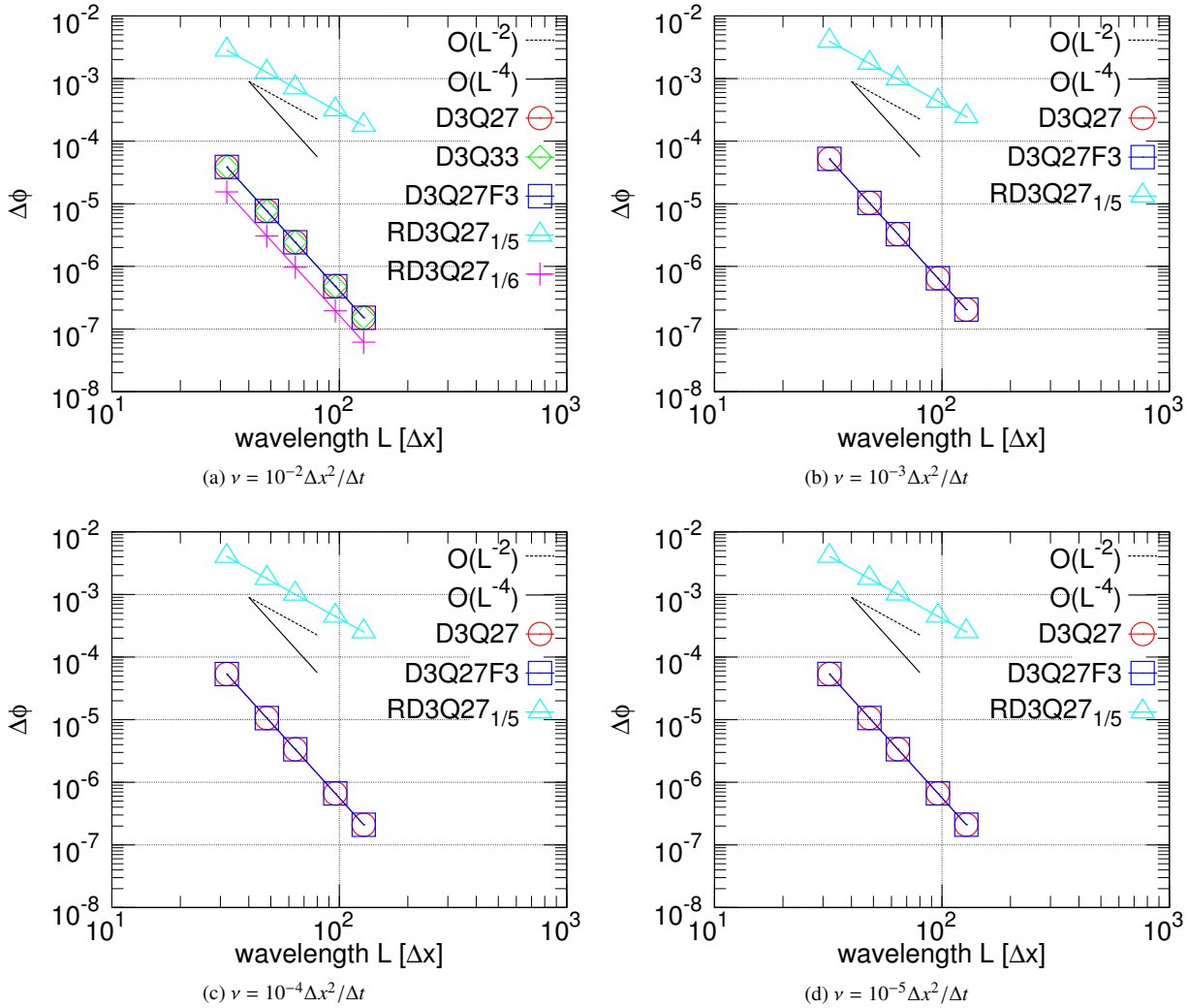

(a) $\nu = 10^{-2}\Delta x^2/\Delta t$

(b) $\nu = 10^{-3}\Delta x^2/\Delta t$

(c) $\nu = 10^{-4}\Delta x^2/\Delta t$

(d) $\nu = 10^{-5}\Delta x^2/\Delta t$

Figure 6: Phase error for the traveling double shear wave as in Fig. 5 but with advection velocity $u_0 = 0.01\Delta x/\Delta t L_0/L$. The results are consistent with the results obtained at the higher velocity. It is of note that reducing the velocity by a factor of ten does not improve the poor stability of the RD3Q27$_{1/6}$ and the D3Q33 method significantly. As in the traveling Taylor-Green vortex, the magnitude of the phase shift error is not a strong function of viscosity.

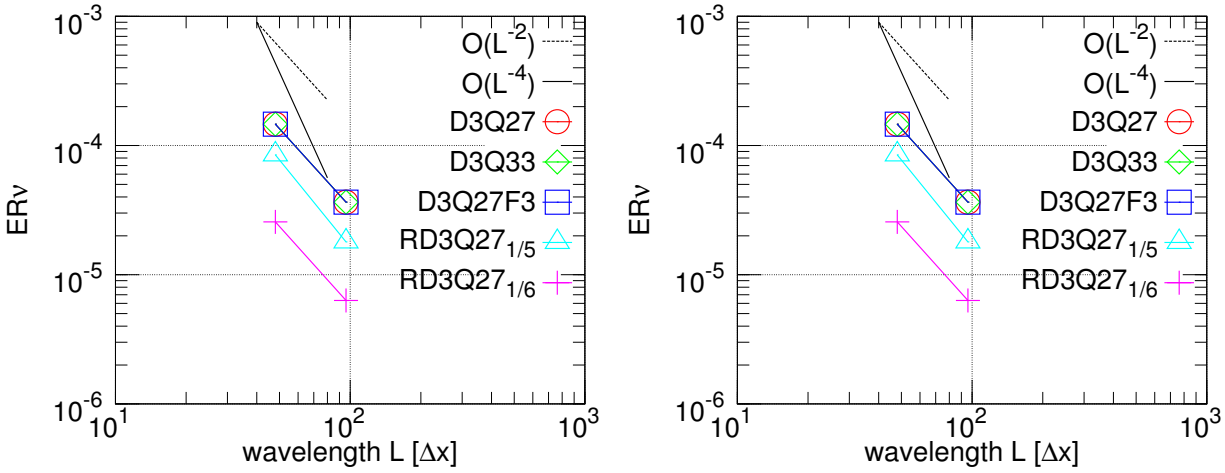

(a) $\nu = 10^{-2}\Delta x^2/\Delta t$

(b) $\nu = 10^{-3}\Delta x^2/\Delta t$

(c) $\nu = 10^{-4}\Delta x^2/\Delta t$

(d) $\nu = 10^{-5}\Delta x^2/\Delta t$

Figure 7: ToBeRemoved

View publication stats